EUROPHYSICS LETTERS 20 November 1996

Europhys. Lett., **36** (6), pp. 419-424 (1996)

Self-focusing and soliton formation in media with anisotropic nonlocal material response

A. A. Zozulya[1], D. Z. Anderson[1], A. V. Mamaev[2](*) and M. Saffman[2]

[1] *JILA, University of Colorado - Boulder, CO 80309-0440, USA*
[2] *Department of Optics and Fluid Dynamics, Risø National Laboratory Postbox 49, DK-4000 Roskilde, Denmark*

(received 28 June 1996; accepted in final form 4 October 1996)

PACS. 42.65Tg – Optical solitons; nonlinear guided waves.
PACS. 42.65Jx – Beam trapping, self-focusing, and thermal blooming.
PACS. 42.65Hw – Phase conjugation, optical mixing, and photorefractive effect.

Abstract. – We investigate self-focusing in bulk media with anisotropic nonlocal photorefractive response. Analytical results demonstrate the possibility of the existence of anisotropic soliton solutions. Self-focusing of Gaussian beams and their convergence to elliptically shaped soliton solutions is investigated theoretically and demonstrated experimentally.

In typical nonlinear optical media the material responds to the presence of the optical field $B(\mathbf{r})$ by a nonlinear change in its refractive index δn that is an algebraic (local) function of the light intensity. This local response in its simplest case $\delta n \propto |B|^2$ results in the canonical nonlinear Schrödinger equation for the amplitude of light propagating in the medium [1]. Higher-order nonlinearities result in various forms of local saturable response [2]. In photorefractive media the change in the refractive index is proportional to the amplitude of the static electric field induced by the optical beam. Finding the material response therefore requires solving globally an elliptic-type equation for an anisotropic electrostatic potential with a source term due to light-induced generation of mobile carriers [3] that has no direct analogs in nonlinear optics. The closest structurally similar counterparts probably are Davey-Stewartson equations [4] describing nonlinear dispersive waves in fluid dynamics or Zakharov equations for parametrically coupled electromagnetic and Langmuir waves in plasmas [5].

Media with a photorefractive nonlinearity turn out to be convenient for studying complex spatial dynamics. These include formation of patterns [6], self-focusing [7], [8], and transverse modulation instability of solitary stripe beams [9] with formation of optical vortices [10]. In this work we present the theory of steady-state two-transverse-dimensional solitons in bulk media with nonlocal anisotropic photorefractive response and analyze their properties in detail. Evolution of arbitrary Gaussian beams, their convergence to elliptically shaped

(*) Permanent address: Institute for Problems in Mechanics, Russian Academy of Sciences, Prospekt Vernadskogo 101, Moscow, 117526 Russia.

soliton asymptotic states, the rate of this convergence, and its dependence on the parameters of the problem are investigated both numerically and experimentally.

Propagation of an optical beam $B(\mathbf{r})$ in a photorefractive medium is governed by the set of equations [3], [9], [10]

$$\left[\frac{\partial}{\partial x} - \frac{i}{2}\nabla^2\right] B(\mathbf{r}) = i\frac{\partial\varphi}{\partial z} B(\mathbf{r})\,, \tag{1a}$$

$$\nabla^2\varphi + \nabla \ln(1+|B|^2)\cdot\nabla\varphi = \frac{\partial}{\partial z}\ln(1+|B|^2)\,. \tag{1b}$$

Here $\nabla = \hat{y}(\partial/\partial y) + \hat{z}(\partial/\partial z)$ and φ is the dimensionless electrostatic potential induced by the beam with the boundary conditions $\nabla\varphi(\mathbf{r}\to\infty)\to 0$. The dimensionless coordinates (x,y,z) are related to the physical coordinates (x',y',z') by the expressions $x=\alpha x'$ and $(y,z)=\sqrt{k\alpha}(y',z')$, where $\alpha = (1/2)kn^2 r_{\text{eff}} E_{\text{ext}}$. Here k is the wave number of light in the medium, n is the index of refraction, r_{eff} is the effective element of the electro-optic tensor, and E_{ext} is the amplitude of the external field directed along the z-axis far from the beam. The normalized intensity $|B(\mathbf{r})|^2$ is measured in units of saturation intensity I_d, so that the physical beam intensity is given by $|B(\mathbf{r})|^2 I_d$. Equations (1) are valid for relatively wide beams and neglect the part of the nonlinearity responsible for asymmetric stimulated scattering since it is not important in the range of parameters discussed here (for details see [3]). For typical spatial structures of light in the conditions when this second part dominates see [11].

The strong anisotropy of eqs. (1) does not allow radially symmetric solutions. In the simplest approximation the beam should be treated as elliptical and characterized by two diameters d_y and d_z along the y and z axes, respectively. Its amplitude in the parabolic approximation can be expressed in the form

$$B = \sqrt{I_{\text{m}}}\exp\left[-\frac{4y^2}{d_y^2} - \frac{4z^2}{d_z^2} + i\frac{y^2}{2}\frac{d_y'}{d_y} + i\frac{z^2}{2}\frac{d_z'}{d_z} + i\theta\right], \tag{2}$$

where $I_{\text{m}} = I_{\text{in}} d_y(0) d_z(0)/d_y d_z$ and $\theta(x)$ is the nonlinear phase change. The primes denote differentiation with respect to x. In the unsaturated regime $I_{\text{m}} \le 1$ eq. (1b) reduces to $\nabla^2\varphi = \partial|B(\mathbf{r})|^2/\partial z$. Its solution in cylindrical coordinates $y = r\cos\psi, z = r\sin\psi$ takes the form

$$\varphi(r,\psi) = \frac{I_{\text{m}}}{16 d_z^2}\sum_{k=0}^{\infty} r^{2k+1} F_k(r^2)\sin(2k+1)\psi\,, \tag{3a}$$

$$F_k = \int_{\infty}^{r^2} \mathrm{d}\tau\,\tau^{-2k-2}\int_0^{\tau}\mathrm{d}\tau'\,\tau'^{k+1} A_k(\tau')\exp[-a\tau']\,, \tag{3b}$$

$$A_k = (-1)^{k+1}\left[\delta_{k,0} + (1-\delta_{k,0})I_k(b\tau) + I_{k+1}(b\tau)\right]. \tag{3c}$$

Here $a = 4(d_y^{-2} + d_z^{-2})$, $b = 4(d_y^{-2} - d_z^{-2})$, and I_k are modified Bessel functions. The refractive index in the central region of the beam according to eqs. (3) is given by the expression

$$\nu(y,z) = -8 I_{\text{m}}\frac{d_z^2 y^2 + (d_y^2 + 2d_y d_z)z^2}{d_z^2(d_y + d_z)^2}\,. \tag{4}$$

Substituting expressions (4) and (2) into eq. (1a), one arrives at the set of equations [12]

$$d_y'' = 16 d_y^{-3}\left[4 - \kappa F^3 (F+1)^{-2}\right], \quad d_z'' = 16 d_z^{-3}\left[4 - \kappa(F+2)(F+1)^{-2}\right], \tag{5}$$

where $\kappa = I_{\text{in}} d_y(0) d_z(0)$ and $F = d_y(x)/d_z(x)$ is the beam diameter ratio. Equations (5) demonstrate a nontrivial nonseparable way in which both diameters of the beam contribute

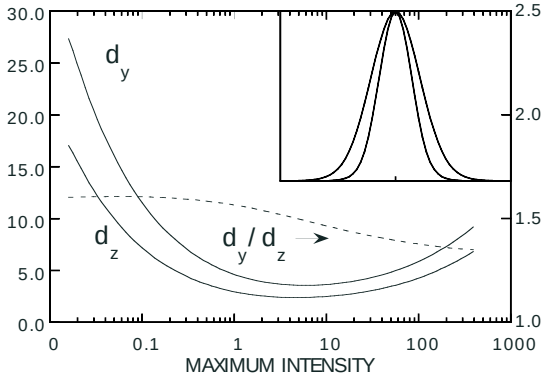

Fig. 1.

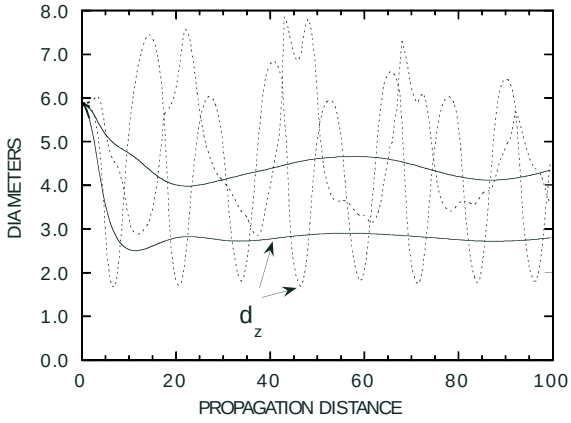

Fig. 2.

Fig. 1. – Diameters of the soliton solution of eq. (1) and their ratio *vs.* its maximum intensity. The insert shows the soliton intensity cross-sections for $I_{\mathrm{m}} = 5$.

Fig. 2. – Evolution of diameters of an initially round Gaussian beam for $I_{\mathrm{in}} = 0.5$ (solid) and 6 (dashed curves).

to its evolution. In particular they show the possibility of a self-channeled propagation $d_y, d_z = \mathrm{const}$ that corresponds to the value of the diameter ratio F determined by the relation $F^3 = F + 2$ or $F = F_0 \approx 1.5$. The self-channeled beam is narrower in the direction of the applied field and wider in the perpendicular direction. Stability analysis reveals that the evolution of perturbations around this solution is of an oscillatory character in the framework of an aberrationless approximation.

The analytical results indicate that eqs. (1) may have soliton solutions $B(x, y, z) = b(y, z) \exp[i\lambda x]$, where λ is a real propagation constant. These solutions have been found numerically by iteratively solving eqs. (1) using the renormalisation procedure due to Petviashvili [13]. Note that this approach is exact and does not imply any approximations (*e.g.*, a Gaussian ansatz) made previously in the theoretical treatment. The lowest-order soliton solution of eqs. (1) turns out to be a smooth one-humped beam that is narrower along the coordinate z and wider in the perpendicular direction.

Figure 1 shows the diameters d_y and d_z of the soliton solution and their ratio d_y/d_z as functions of the soliton maximum intensity $I_{\mathrm{m}} = |b(0, 0)|^2$. The diameters have been calculated at the 1/2 level of the maximum intensity. The insert presents the cross-sections of the soliton intensity for $I_{\mathrm{m}} = 5$ along the z (narrower curve) and the y (wider curve) axes. The values of the diameters are inversely proportional to the square root of the soliton maximum intensity $d_{y,z} \propto 1/\sqrt{I_{\mathrm{m}}}$ for $I_{\mathrm{m}} \to 0$, logarithmically proportional to it ($d_{y,z} \propto \sqrt{\ln I_{\mathrm{m}}}$) in the opposite limit $I_{\mathrm{m}} \to \infty$, and pass through shallow minima in between. Notice that the diameter ratio in fig. 1 is strikingly close to that given by the analytical formulas, eq. (5). The absolute values of the diameters for $I_{\mathrm{m}} \leq 1$ are about two times off.

Numerical analysis of the evolution of arbitrary initial beams indicates that the soliton solutions are attractors of the set of eqs. (1). The rate of convergence to these solutions depends primarily on the normalized intensity I_{m}. We have found that evolution of an input beam in general is characterised by oscillations of both its diameters, in qualitative agreement with the results of the analytical approach. In the unsaturated limit $I_{\mathrm{m}} \ll 1$ these oscillations are strongly damped and their spatial period scales as $1/I_{\mathrm{m}}$. The initially round beam becomes

elliptical and converges to the soliton solution. Increasing $I_{\rm m}$ up to about unity decreases the period of the oscillations, while still keeping them reasonably heavily damped, thereby decreasing the length of the spatial transient. Further increase in $I_{\rm m}$ up to several units still decreases the spatial period of oscillations but also sharply decreases the relaxation rate and increases the spatial transient length. In the very high-saturation regime (roughly $I_{\rm m} > 50$) the oscillation period starts to grow and the relaxation rate remains small, so the spatial transient length remains large. The characteristic period of oscillations in this case may exceed the length of the medium. By adjusting input parameters the output profiles of the beam in the high-saturation transient regime can be made to have a broad range of shapes starting from beams that are more elongated along the y-axis to those elongated along the z-axis and including round output beams in between.

Figure 2 shows spatial evolution of the input Gaussian beam $B_{\rm in} = \sqrt{I_{\rm in}} \exp[-2 \ln 2 (r/d)^2]$ for $I_{\rm in} = 0.5$ (solid) and 6 (dashed curves). Inside the medium the beam undergoes self-focusing and its intensity $I_{\rm m}$ becomes ≈ 1.1 and 7–27, respectively. Note the rapid relaxation to the soliton solution for $I_{\rm in} = 0.5$ and a very long transient in the high-saturation regime. Note also that the longitudinal span of fig. 2 considerably exceeds the characteristic lengths of photorefractive media, concrete estimates will be given below. Figure 2 demonstrates that the best parameter region to observe solitons corresponds to a moderate-saturation regime when the intensity of the beam is about the saturation intensity. In the unsaturated limit $I_{\rm m} \ll 1$ the oscillations of an input beam are damped but the overall evolution scale goes up as $1/I_{\rm m}$. In the high-saturation regime $I_{\rm m} \gg 1$ the damping rate is too small and the spatial transients last a very long distance.

The experimental arrangement was similar to that used in ref. [9], [10]. A 10 mW He-Ne laser beam ($\lambda = 0.63$ μm) was passed through a variable beam splitter and a system of lenses controlling the size of the beam waist. The beam was directed into a photorefractive crystal of SBN:60 doped with 0.002% by weight Ce. The beam propagated perpendicular to the crystal $\hat{c}$-axis, and was polarized along it to take advantage of the largest component of the electro-optic tensor of SBN r_{33}. The crystal measured 10 mm along the direction of propagation, and was 9 mm wide along the $\hat{c}$-axis. A variable dc voltage was applied along the $\hat{c}$-axis to control the value of nonlinear coupling. Images of the beam at the output face of the crystal were recorded with a CCD camera. The diameters were measured from scans of the output images at the 1/2 level of the maximum intensity. The effective saturation intensity was varied by illuminating the crystal from above with incoherent white light. The dependence of the photorefractive coupling constant on saturation intensity $I_{\rm d}$ in the absence of an applied field takes the form [14] $\gamma = \gamma_0 I_{\rm beam}/(I_{\rm beam} + I_{\rm d})$. By measuring the two-beam coupling gain with the white-light source off ($I_{\rm d} = 0$) and on ($I_{\rm d} \neq 0$) the ratio $I_{\rm m} = I_{\rm beam}/I_{\rm d}$ has been determined.

Experiments in the high-saturation regime $I_{\rm m} \gg 1$ showed that the shape of the input round beam at the output from the nonlinear medium changes as a function of the voltage, the input diameter of the beam, and the focusing conditions. At high voltages the center of the output beam was also displaced along the $\hat{c}$-axis by up to a couple of beam diameters due to self-bending [3]. We have observed ellipticities d_y/d_z ranging from about 0.5 to 5, including round output beams. This is illustrated in fig. 3 which shows the output diameters of the round input 26 μm diameter beam as functions of the applied voltage in the high-saturation regime. The inserts show the beam profile at 0.5 and 0.9 kV. Note how the beam diameter ratio value d_y/d_z flips over between 0.4 and 0.7 kV and then reverts to values larger than unity.

Recent experimental observations of photorefractive self-focusing in two transverse dimensions have claimed that solitons have cylindrical symmetry [8]. Our results contradict this

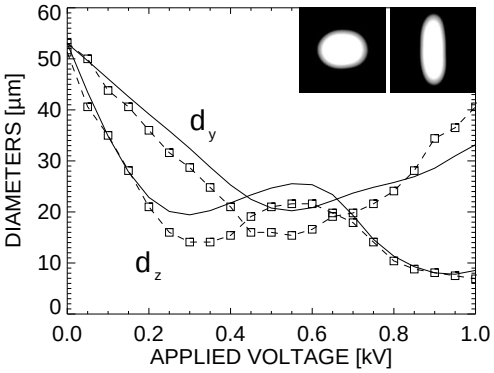

Fig. 3.

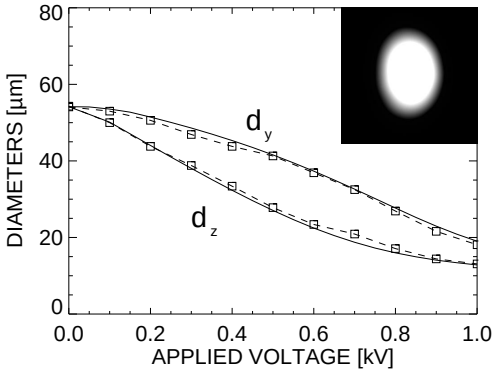

Fig. 4.

Fig. 3. – Ouput diameters *vs.* applied voltage in the high-saturation regime. The power of the input beam was 50 μW.

Fig. 4. – Ouput diameters *vs.* applied voltage in the moderate-saturation regime. The power of the input beam was 4.2 μW.

claim and we believe that the results in ref. [8] should be identified as a transient stage of convergence to a soliton. As a proof of their claim the authors of ref. [8] presented a side-view image of the beam passing through the crystal and several beam profiles at distances up to 0.7 mm apart, that, according to the authors, showed the same beam diameters. The technique of imaging through the nonlinear medium has been characterized in ref. [7] as "not valid" due to high uncontrollable distortions. As concerns the profiles, the corresponding FWHM diameters measured from the data in the last of ref. [8] turn out to vary by about 25% (from 10.7 μm to 13.3 μm). The experiments were conducted in the high-saturation regime where the evolution of a light beam is accompanied by long transient oscillations. According to our estimates the spatial period of these oscillations was slightly larger than the size of the crystal. By an appropriate choice of parameters (see fig. 3) the output beam diameter ratio can be made to have many values (in particular, be equal to unity). The deviations from a round shape at distances of about 0.7 mm should be about plus/minus ten percent, which is in good agreement with the experimental data of ref. [8].

Figure 4 shows the output diameters *vs.* the applied voltage for the same beam as in fig. 3 but with twelve times smaller power. It demonstrates rapid convergence of the output beam profile to an elliptical shape elongated along the y-axis characteristic for the soliton solution. The insert is the output intensity distribution for 1.0 kV external voltage. The measured normalized input beam intensity for fig. 4 was $I_{\mathrm{m}} \approx 0.6$ with about 30% uncertainty. In fig. 3 the laser power was set 12 times higher than in fig. 4, so the value of I_{m} in fig. 3 is known to be 12 times higher than in fig. 4 with high accuracy. The measured value of the electro-optic coefficient for our crystal is $r_{33} = 360$ pm/V. Solid curves in fig. 3 and 4 are theoretical comparisons obtained by solving eqs. (1) with a 26 μm diameter collimated input Gaussian beam and $I_{\mathrm{m}} = 6$ and 0.5, respectively. Note that the only parameter in the theoretical calculations with a relatively large experimental uncertainty was I_{m} in fig. 4, which was chosen to give the best agreement with the data. The resulting agreement for both figures, considering the complexity of the system being modelled, is strikingly good. Quantitative differences in fig. 3 are probably due to the non-Gaussian shape of the beam and some uncertainty in the position of its waist with respect to the crystal face.

For the above parameters and 1.0 kV voltage the 26 μm input diameter translates to 5.8 in units of fig. 2 and the one-centimeter crystal length to the propagation distance $x \approx 22$–23. Solid and dashed curves in fig. 2 in the range $0 < x < 23$ show the evolution of the beam diameters inside the crystal for the 1.0 kV/cm points in fig. 3 and 4, respectively. As is seen from fig. 2 the spatial transients at the output from the crystal for $I_{\text{in}} = 0.5$ are largely gone and the beam is close to its asymptotic soliton shape. This allows us to conclude that data in fig. 4 present experimental observation of convergence to the soliton solutions found in this paper.

***

AAZ and DZA acknowledge the support of NSF grant PHY90-12244 and the Optoelectronics Computing Center, an NSF Engineering Research Center. The work at Risø was supported by the Danish Natural Science Research Council.

REFERENCES

[1] Chiao R. Y., Garmire E. and Townes C. H., *Phys. Rev. Lett.*, **13** (1964) 479.

[2] Marburger J. H., *Prog. Quantum Electron.*, **4** (1975) 35; Karlsson M., *Phys. Rev. A*, **46** (1992) 2726; Suter D. and Blasberg T., *Phys. Rev. A*, **48** (1993) 4583; Dowell M. *et al.*, *Phys. Rev. A*, **52** (1995) 3244.

[3] Zozulya A. A. and Anderson D. Z., *Phys. Rev. A*, **51** (1995) 1520.

[4] Ablowitz M. J. and Segur H., *Solitons and the Inverse Scattering Transform* (SIAM, Philadelphia) 1981.

[5] Zakharov V. E., *Zh. Èksp. Teor. Fiz.*, **62** (1972) 1745 (*Sov. Phys. JETP*, **35** (1972) 908).

[6] Honda T., *Opt. Lett.*, **18** (1993) 598; Mamaev A. V. and Saffman M., *Europhys. Lett.*, **34** (1996) 669.

[7] Iturbe-Castillo M. D. *et al.*, *Appl. Phys. Lett.*, **64** (1994) 408; Iturbe-Castillo M. D. *et al.*, *Opt. Commun.*, **118** (1995) 515.

[8] Duree G. *et al.*, *Phys. Rev. Lett.*, **71** (1993) 533; Shih M.-F. *et al.*, *Electron. Lett.*, **31** (1995) 826; Shih M.-F. *et al.*, *Opt. Lett.*, **21** (1996) 324.

[9] Mamaev A. V., Saffman M. and Zozulya A. A., *Europhys. Lett.*, **35** (1996) 25; Mamaev A. V., Saffman M., Anderson D. Z. and Zozulya A. A., *Phys. Rev. A*, **54** (1996) 870.

[10] Mamaev A. V., Saffman M. and Zozulya A. A., *Phys. Rev. Lett.*, **76** (1996) 2262.

[11] Zozulya A. A., Saffman M. and Anderson D. Z., *Phys. Rev. Lett.*, **73** (1994) 818.

[12] Zozulya A. A. and Anderson D. Z., in *Proceedings of the International Conference on Photorefractive Materials, Effects and Devices*, edited by D. Z. Anderson and J. Feinberg (Estes Park) 1995, p. 399.

[13] Petviashvili V. I., *Fiz. Plazmy*, **2** (1976) 469 (*Sov. J. Plasma Phys.*, **2** (1976) 257).

[14] Kukhtarev N. V. *et al.*, *Ferroel.*, **22** (1979) 949.